AGU
ADVANCING
EARTH AND
SPACE SCIENCE

Geophysical Research Letters®

Key Points:

- A linear inverse model is used to quantify the natural variability in the El Niño/Southern Oscillation-southwest United States (ENSO-SWUS) teleconnection, and it suggests considerable intrinsic variability
- This natural variability demonstrates that detecting anthropogenic changes in the ENSO-SWUS hydroclimate teleconnection will be difficult
- CMIP6 shows an improvement in modeling the ENSO-SWUS teleconnection, but uncertainty remains in the projected future climate

Intrinsic Century-Scale Variability in Tropical Pacific Sea Surface Temperatures and Their Influence on Western US Hydroclimate

Colin P. Evans[1] , Sloan Coats[2], Carlos M. Carrillo[1], Xiaolu Li[1] , Marc J. Alessi[3] ,
Dimitris A. Herrera[4], Brandon N. Benton[5], and Toby R. Ault[1]

[1]Department of Earth and Atmospheric Science, Cornell University, Ithaca, NY, USA, [2]Department of Earth Sciences, University of Hawai'i at Mānoa, Honolulu, HI, USA, [3]Department of Atmospheric Science, Colorado State University, Fort Collins, CO, USA, [4]Department of Geography and Sustainability, The University of Tennessee-Knoxville, Knoxville, TN, USA, [5]National Renewable Energy Lab, U.S. Department of Energy, Washington, DC, USA

Abstract Hydroclimate variability of the southwest United States (SWUS) is influenced by the tropical Pacific Ocean, particularly through the teleconnection to El Niño/Southern Oscillation (ENSO), which is expected to be altered by climate change. Natural variability in this teleconnection has not been robustly quantified, complicating the detection of anthropogenic climate change. Here, we use a linear inverse model (LIM) to quantify natural variability in the ENSO-SWUS teleconnection. The LIM yields realistic teleconnection patterns with century-scale variability comparable to simulations from the Last Millennium Ensemble project and the Climate Model Intercomparison Project Phases 5 and 6. The variability quantified by the LIM illuminates two aspects of our understanding of ENSO and its impacts: the inherent statistics of the observable system can produce century-long periods with a wide range of correlations to SWUS hydroclimate, including nonsignificant correlations, and thus that detecting changes in ENSO-related hydroclimate variability is challenging in a changing climate.

Plain Language Summary The El Niño/Southern Oscillation (ENSO) affects weather and climate across the globe through teleconnections. For example, when sea surface temperatures in the tropical Pacific Ocean are warmer than normal (e.g., during an El Niño), higher than normal precipitation is typically observed in the southwest United States (SWUS). However, because we have temporally limited observations of climate, we do not know how often El Niños *actually* bring more rain to the SWUS. Assessing this natural variability is difficult with commonly used approaches from the climate sciences. Here, we use a statistical model to emulate the characteristics of ENSO teleconnections from observations. Doing so demonstrates that there is considerable natural variability in the ENSO teleconnection to the SWUS. This suggests that even though ENSO and its impact on weather and climate are expected to change due to climate change, detecting such changes will be difficult.

1. Introduction

Much of the southwestern United States has been in some form of drought for at least the last two decades (NADM, 2022), and water supplies continue to decline in the region (Williams et al., 2022). The El Niño/Southern Oscillation (ENSO) is the primary driver of interannual hydroclimate variability in the southwest United States (SWUS, 32–40°N, 120–105°W, Figure 1b), wherein El Niño (La Niña) brings anomalously high (low) amounts of rain to the region (Cook et al., 2018; Redmond & Koch, 1991). Despite the importance of the ENSO teleconnection to the SWUS hydroclimate, we lack a clear picture of its stability.

ENSO is the dominant source of interannual variability in the tropical Pacific Ocean with observable teleconnections to many other parts of the globe (Hoerling et al., 1997). Despite the abundance of research into this phenomenon and its teleconnections (e.g., Alexander, et al., 2002; Cai et al., 2020; Deser et al., 2017; Gupta & Jain, 2021), there are important aspects of ENSO that remain unknown, like its role in a changing climate (Yang et al., 2018). For instance, Yeh et al. (2018) examined general circulation models (GCMs) from both the Coupled Model Intercomparison Project Phase 3 and 5 (CMIP3 and CMIP5) and found that they do not yield a consistent picture of how ENSO and its teleconnections will change during the 21st century. While some studies have found consistent changes for a subset of these GCMs and the most extreme of ENSO events (Cai et al., 2018), others
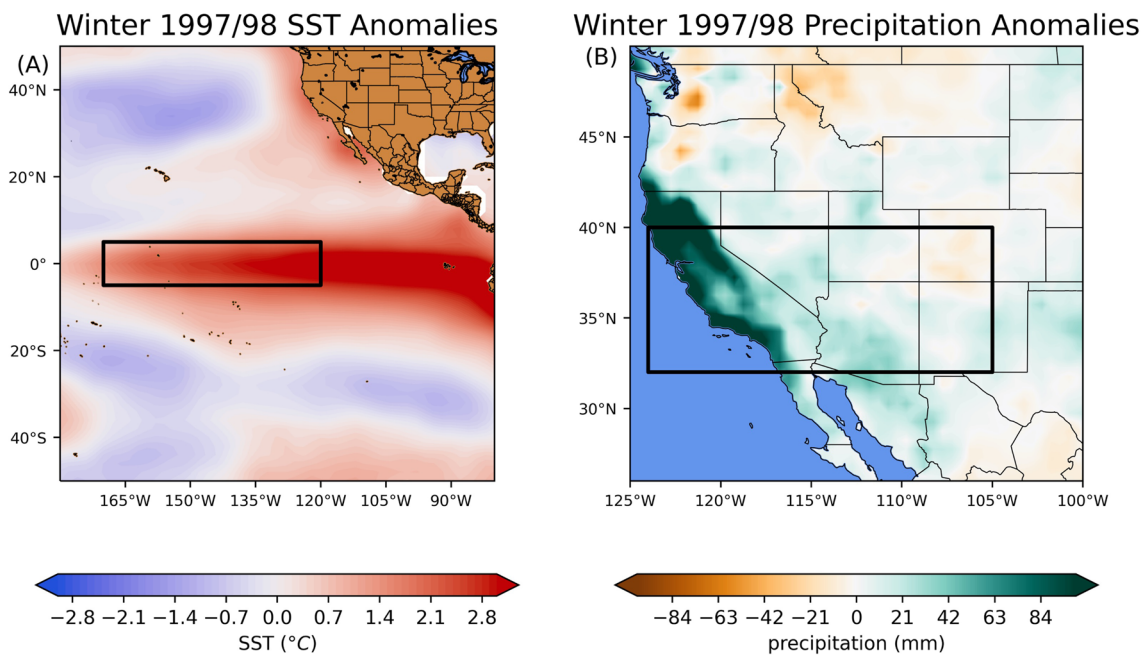
Figure 1. A "typical" El Niño/Southern Oscillation teleconnection to the southwest United States, with (a) winter (DJF) sea surface temperature (SST) anomalies against the 1951–1980 climatology using Extended Reconstructed SST V3b in the color contours, and the Niño3.4 region within the Pacific Ocean, covering 5°S–5°N and 170–120°W in the box, and (b) the southwestern United States with a box over the specific study area covering 32–40°N and 120–105°W, with precipitation anomalies against the 1951–1980 climatology using GPCC gridded data (Schneider et al., 2011) in the color contours.

have identified a close relationship between mean state biases in these GCMs and their responses to anthropogenic climate change (Stevenson et al., 2021). The simulated strength and spatial pattern of ENSO teleconnections in our current climate varies considerably across GCMs (Langenbrunner & Neelin, 2013; Weare, 2013; Yeh et al., 2018). The biases in ENSO within the GCMs include too much sea surface temperature (SST) variability, a weak annual cycle, and El Niños that propagate too far eastward from what is observed (Chen et al., 2017; Jiang et al., 2021). Even when SST anomalies in GCMs are nudged toward observations, composite ENSO events in an ensemble of GCMs showed considerable teleconnection variability (Deser et al., 2017). And because of the short length of observational records, we do not have a sufficient real-world baseline against which to compare these GCMs (Deser et al., 2010, 2017).

ENSO is an important source of seasonal predictability in the SWUS hydroclimate, and yet observed precipitation responses can be inconsistent between individual events, including the sign of the precipitation anomalies (Hoerling & Kumar, 2002). Most recently, the 2015/2016 El Niño, despite being one of the strongest in the observational record (Zhai et al., 2016), did not result in wetter conditions across the SWUS, and thus many areas of the region, especially Southern California, remained in severe drought conditions (Cash & Burls, 2019). The presence of significant inter-event differences in ENSO and its impact also suggests that internal atmospheric variability alone can modulate ENSO teleconnections (Zhang et al., 2018). For instance, Chen and Kumar (2018) analyzed ensemble forecasts for the 2015/2016 winter season and found large differences in forecasted winter precipitation for the SWUS between ensemble members of the NCEP operational Climate Forecast System, version 2 (NCEP, 2019). Cash and Burls (2019) found that ensemble means often show the SWUS hydroclimate is over-modulated by ENSO and that the hydroclimate is dominated by internal variability. Furthermore, other modes of variability and external forcing can act as a modulating force on ENSO teleconnections, such as the Pacific Decadal Oscillation (Gershunov & Barnett, 1998; Singh et al., 2021), the Atlantic Multidecadal Oscillation (Enfield et al., 2001; McCabe et al., 2004), and the North Atlantic Oscillation (Rajagopalan et al., 2000), all of which can reduce or enhance ENSO's teleconnections to the SWUS. Similarly, Li et al. (2019) and Larson et al. (2022) both found that the Pacific-North American pattern has significant variability not associated with ENSO, indicating another mode of internal atmospheric variability that can act as a modulating force on ENSOs teleconnections.

Previous research into the stability of ENSO teleconnections have used GCMs, the paleoclimate record, or relied on the limited observational record. For instance, Coats et al. (2013) found a high amount of temporal variability in ENSO teleconnection strength between winter (DJF) tropical Pacific SSTs and DJF 200-mb geopotential heights over North America in the control runs of CMIP5. In forced transient simulations from the same GCMs, a similar level of temporal variability in ENSO teleconnections was found (Lewis & LeGrande, 2015). However, results also showed that the spatial features of the teleconnections vary considerably across GCMs (Coats et al., 2013; Langenbrunner & Neelin, 2013), with implications for the real-world relevance of these results. Likewise, within observational records, it has been suggested that ENSO teleconnections vary in both space and time, although these results are limited to shorter timescales of variability (e.g., Cole & Cook, 1998; Gershunov & Barnett, 1998; Hu & Feng, 2001; Rajagopalan et al., 2000). Deser et al. (2018) showed that ENSO teleconnection strength can range more than twofold in certain locations.

The observed ENSO-SWUS correlation is just one number out of a range of plausible correlations that are consistent with the dynamics of the climate system. Despite the attempts referenced above, robustly defining this range is complicated. For instance, the range of correlation estimated from GCMs varies from model to model and from century to century in some GCMs (Langenbrunner & Neelin, 2013; Lewis & LeGrande, 2015). Additionally, GCMs have many biases that can preclude their relevance to understanding climatic phenomena in the real world (Coats et al., 2013). Adding a further complication, there is now debate on how to handle the "hot model problem," wherein some models included in CMIP6 are predicting rising temperatures that are not supported by observations and that using these models may skew results (Hausfather et al., 2022), which is an important consideration when examining ENSO teleconnections. We therefore do not have a reliable benchmark for the distribution of realistic correlation values given what we know about the system over the historical period.

To address these issues, following the work of Ault et al. (2018), we use a Linear Inverse Model (LIM) to characterize variations in ENSO-SWUS teleconnection. LIMs have been applied to examine and determine the significance of low frequency variability in the tropical Pacific on decadal timescales (Ault, Deser, et al., 2013), the significance of "Modoki" El Niño events (Newman et al., 2011), determine the predictability of the Pacific Decadal Oscillation (Newman et al., 2016), and to test the significance of tropical Pacific SST gradient trends relative to internal variability (Coats & Karnauskus, 2017). Other studies have utilized a LIM to make seasonal ENSO predictions (Penland & Sardeshmukh, 1995), and to evaluate the ability of GCMs to make decadal forecasts (Newman, 2013). Additionally, the LIM has been shown to successfully reproduce ENSO and PDO statistics and can outperform certain forecast models (Perkins & Hakim, 2020) and it has been used to predict Pacific SST anomalies (Alexander et al., 2008). Herein, we use the LIM to provide a robust characterization of the range of correlations that are consistent with the observational record. We then use this range as a benchmark against which to compare GCM ensembles from the Last Millennium Ensemble (LME), CMIP5, and CMIP6.

2. Data and Methodology

2.1. Constructing the LIM

We build upon the LIM used by Penland and Matrosova (1994) and Penland and Sardeshmukh (1995), and more recently that of Ault et al. (2018) and Coats et al. (2020), with some specific changes to its construction to emulate the inherent statistics found in an observational data set. First, SST anomalies were calculated using the National Oceanic and Atmospheric Administration (NOAA) Extended Reconstructed SST V3b (Smith et al., 2008), which is a monthly data set of SSTs spanning 1854 to present on a 2° grid. For the SWUS, reconstructions of the Palmer Drought Severity Index (PDSI) are an often-used proxy for drought conditions (e.g., Ault et al., 2018). The observational PDSI input data used was created by Sheffield et al. (2006) and is a 1° resolution monthly data set spanning 1948–2008. Second, to isolate the ENSO and SWUS hydroclimate teleconnection, we restricted the domain of the SST anomalies to that of just the Niño3.4 index and restricted the PDSI to the SWUS.

We ran the LIM for 100,000 years to provide a population of thousand 100-year periods. From there we computed the century-scale correlation values between SWUS PDSI and Niño3.4 SST anomalies for each 100-year period, to produce a range of 1,000 correlation values.
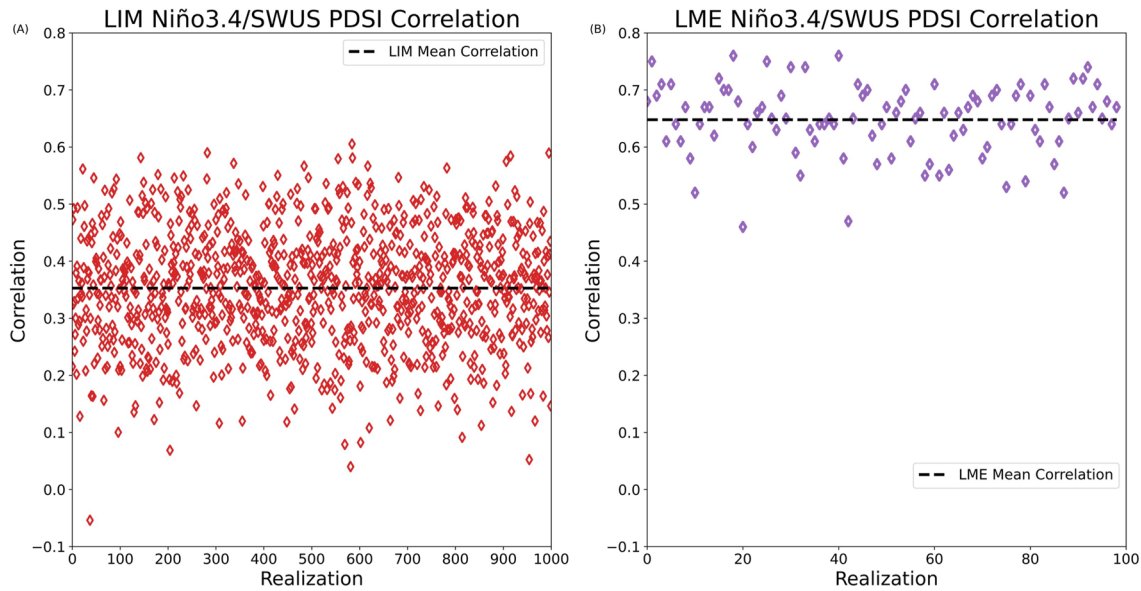
Figure 2. (a) The 1000 the century-long correlation values calculated from the linear inverse model generated Niño3.4 sea surface temperatures (SSTs) and southwest United States (SWUS) Palmer Drought Severity Index (PDSI). The black dotted line is the ensemble mean. (b) Correlation values between Niño3.4 SSTs and SWUS PDSI calculated from 99 distinct century-long periods from the Last Millennium Ensemble (LME) (Methods). The black dotted line is the ensemble mean correlation value from the LME.

2.2. PDSI From Models

As this work follows Ault et al. (2018), and because soil moisture and PDSI are highly correlated in the SWUS (Ault, Cole, et al., 2013) we use PDSI to characterize the hydroclimate of the SWUS, which we calculated offline using available variables from CMIP5, CMIP6, and LME (Otto-Bliesner et al., 2016). LME is a paleoclimate experiment from the National Center for Atmospheric Research offering an ensemble of results covering 850–2006 (Otto-Bliesner et al., 2016). For CMIP5 and CMIP6 we compared the teleconnection strength (Pearson correlation) in the historical experiments to determine if there have been improvements in the simulation of ENSO teleconnections in the new generation of climate models. For CMIP6, we also calculated the teleconnection strength for the newly developed future emissions scenario, Shared Socioeconomic Pathway 585 (SSP585, O'Neill et al., 2016), to quantify changes to ENSO teleconnections due to climate change. For direct comparison to the LIM, we calculate potential evapotranspiration (PET—Allen et al., 1998; Monteith, 1965; Penman, 1948) by utilizing the following variables: net radiation, soil heat flux density, 2-m air temperature, 2-m wind speed, and vapor pressure deficit (Table S1 in Supporting Information S1). A total of 14 models from CMIP5 (Table S2 in Supporting Information S1) and CMIP6 (Table S3 in Supporting Information S1) had the requisite variables needed to calculate PET. We then use precipitation from the models and PET to calculate PDSI. Additional details on calculating PDSI are available in Supporting Information S1. The Pearson correlation value was calculated for each of the CMIP5 and CMIP6 models. For the LME, we binned 99 realizations of the runs to create an ensemble of century-length time series.

3. Results

The LIM suggests that there is a broad empirical distribution (Figure 2a) of correlations that are consistent with observations between 1948 and 2008, and thus considerable natural variability can emerge, even from the relatively stable and short climatic interval sampled by the observational data set. More than 70% of the correlations calculated fell between 0.3 and 0.6, while over 90% fell between 0.2 and 0.6 (Figure 2a) The ensemble mean correlation from the LIM was 0.35, compared to a correlation of 0.37 calculated from the observational data set.

The LME correlation values show a slightly smaller range in teleconnection strength than the LIM, with correlations ranging from 0.45 to 0.75 (Figure 2b). This narrower range is found despite the LME simulating the entire last millennium, and thus also simulating external forcings and long timescale internal variability not sampled by
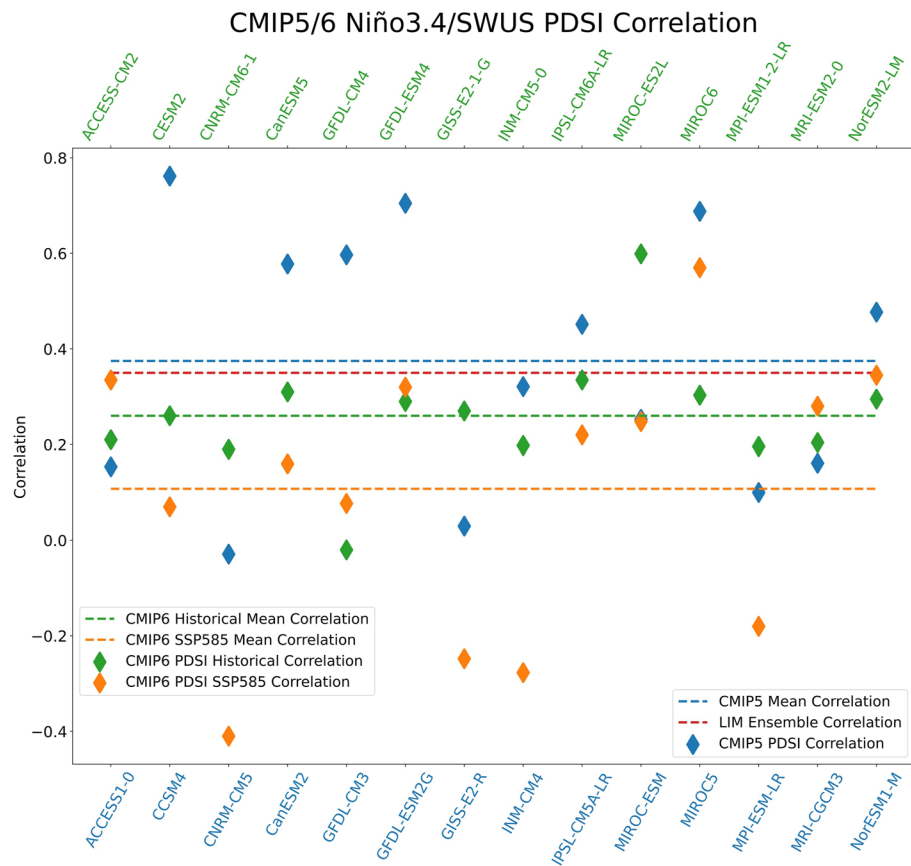
Figure 3. El Niño/Southern Oscillation-southwest United States correlation values calculated from CMIP5 (blue), CMIP6-Historical (green), and CMIP6-SSP585 (orange). The linear inverse model ensemble mean is the dotted red line.

the LIM. Importantly, the ensemble mean correlation from the LME of 0.65 is much greater than that from the LIM, consistent with previous research suggesting that CESM1 (the GCM used in the LME) has an overly strong ENSO teleconnection (e.g., DiNezio et al., 2017). The range of correlations from the LME is narrower than that from the CMIP5 or CMIP6 simulations (Figures 3 and 4), suggesting that inter-GCM structural differences in ENSO teleconnection strength are larger than the natural variability in this metric as simulated by a single model. The ensemble mean correlation from the LME is also higher than that of the CMIP5 or CMIP6 ensembles, and thus overly strong ENSO teleconnections are not a general feature of climate models.

In the CMIP5 simulations, ENSO teleconnections vary in strength, and even in sign, across the models. For instance, CNRM-CM5 exhibits a negative ENSO-SWUS correlation, whereas GFDL-ESM2M exhibits a correlation of over 0.8 (Figure 3). Although the ensemble mean correlation of the CMIP5 simulations was quite close to that from the LIM (0.375 and 0.35, respectively), the range is much wider (Figure 4) and the distribution more uniform. Of relevance to the ability of CMIP5 models to simulate ENSO teleconnection strength, there are five models with correlations below 0.31 (the bottom of the LIM range), indicating too weak of a relationship between Niño3.4 SSTs and SWUS PDSI. Likewise, there are three models with correlations higher than 0.65 (the top of the LIM range), indicating an overemphasis of this relationship.

Overall, the CMIP6 historical simulations exhibit ENSO teleconnection strengths that are more consistent with the LIM as compared to CMIP5 (Figures 3 and 4). While the ensemble mean correlation of 0.26 for the CMIP6 historical simulation is further from the ensemble mean of the LIM, the distribution is narrower, with a range of about 0.0–0.6 for CMIP6 as compared to about −0.1 to 0.8 for CMIP5. Interestingly, there appear to be large changes in teleconnection strength from CMIP5 to CMIP6 for individual modeling centers. For instance, the correlation from GFDL-ESM4 (CMIP6) is a more realistic 0.3 (just inside the LIM range), as compared to 0.7 from GFDL-ESM2G from CMIP5. Likewise, while the NCAR models CESM1 (LME—Figure 2b) and CCSM4
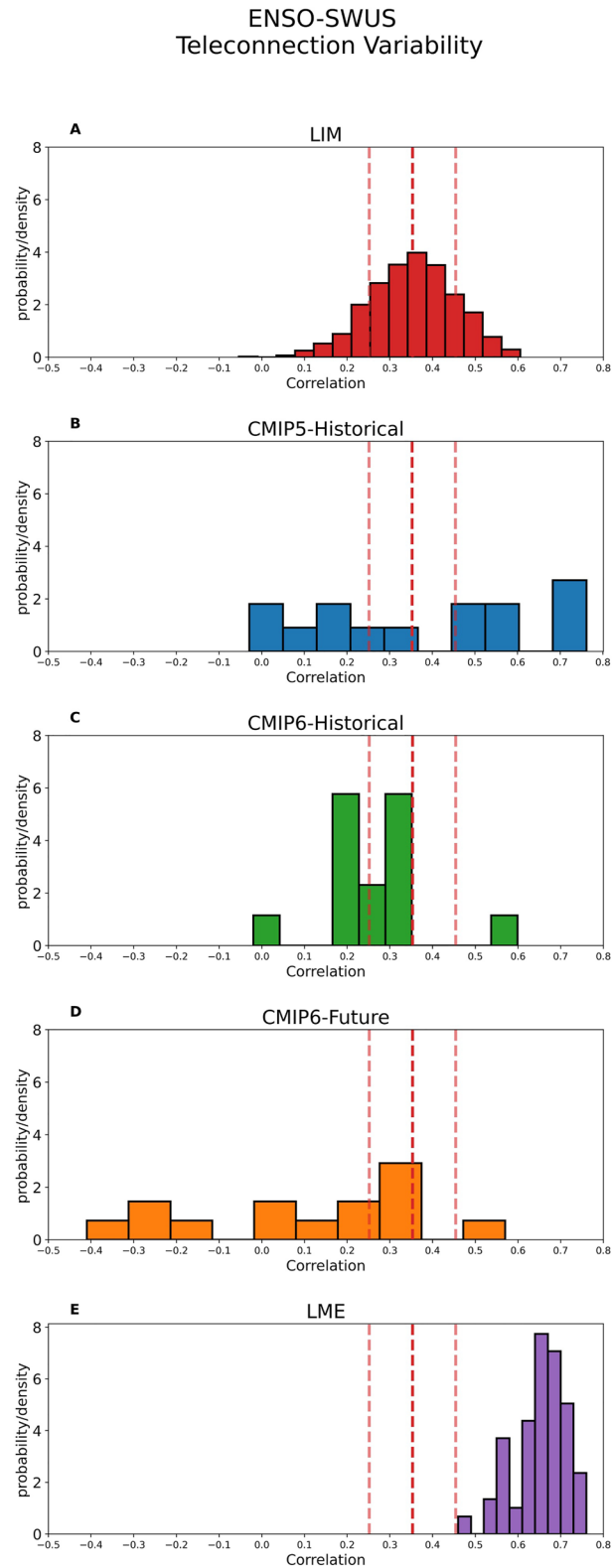
Figure 4. Density/probability plot comparison of El Niño/Southern Oscillation-southwest United States teleconnection strength for the linear inverse model (LIM) (panel (a), red), historical run of CMIP5 (panel (b), blue), CMIP6-Historical (panel (c), green), CMIP6-SSP585 (panel (d), orange), and the Last Millennium Ensemble (panel (e), purple) with the LIM mean (dashed red line) and LIM plus and minus one standard deviations (semi-transparent dashed red line) plotted on each.

(CMIP5—Figure 3) exhibited correlations largely in excess of the LIM, CESM2 (CMIP6—Figure 3) exhibits a correlation that is slightly below the LIM range. Importantly, we also find an overall improvement in the ensemble of CMIP6 models (Figure 3).

Finally, to assess if there are consistent changes in the ENSO teleconnections strength in the future, we also analyzed data from the CMIP6 SSP585 simulations, which are run with a high emissions scenario and thus should exhibit large signal (climate change) to noise (natural variability) ratios. Eight of the 14 simulations exhibit a decrease in the ENSO-SWUS teleconnection strength in the 21st as compared to the 20th centuries (Figure 3), with a change in the ensemble mean correlation from 0.26 to 0.12, respectively. Together, the CMIP6 simulations thus suggest a small but significant decrease in ENSO teleconnection strength in the future. To summarize all of the results, Figure 4 illustrates the ENSO-SWUS teleconnection strength and variability in each of the analyzed ensembles, with a direct comparison of the results between the climate models and the LIM.

4. Discussion

We used a LIM to quantify the natural variability in ENSO-SWUS teleconnections that is expected intrinsically—that is, the range of teleconnection strengths possible given the inherent statistics of an observational data set. Our results exhibit entire centuries of non-significant correlation (roughly 3%–6% of the centuries in the LIM). The LIM does not possess long-term sources of variability, as the output drawn from the LIM relies solely on the 3-month time-lag parameter, calculated from the inherent statistics of the observational data set. Because of this, the LIM samples only a narrow range of plausible behaviors of the system, effectively removing any source of long-term internal or external forcing. Despite this, there are centuries when the Niño3.4 SSTs and SWUS PDSI correlations diminish in significance for purely statistical reasons, indicating that it was not unreasonable to expect ENSO to have had no statistically significant impact on SWUS hydroclimate during the 20th century, like in the results found by Ault et al. (2018). These results are not dissimilar from those of Meehl and Hu (2006) which found SWUS hydroclimate variability in a GCM to be highly irregular. Furthermore, because this result is based entirely on the inherent statistics of the observational data set, it is also not unreasonable to expect a diminished correlation in the future, even without climate change.

The ensemble mean correlation from the LIM was slightly lower than the observational data set on which it was based (0.35 for the LIM compared to 0.37 from observations). While superficially interesting, this was an expected result given that the LIM does not retain 100% of the variance in the Niño3.4 SSTs and the SWUS PDSI, subsequently slightly underemphasizing their relationship. Within the timeframe of the observational data set (1948–2008), there have been seven strong El Niño event. Anomalously higher-than-average PDSI in the SWUS was recorded only after a few of these events (e.g., 1982–1983, 1988–1989, 1998–1999). Therefore, observations alone indicate that not all ENSO events affect the SWUS hydroclimate. Results from the LIM strengthen this conclusion, demonstrating that intrinsic variability is a robust feature of the ENSO-SWUS teleconnection.

This study provides further evidence that tools like the LIM that can be used to assess the ability of GCMs to simulate coupled atmosphere-ocean dynamics, and thus can provide an important benchmark as we subsequently use these GCMs to project climate change.

With such benchmarking in mind, in the LME, the ENSO-SWUS teleconnection is much stronger than in observations or the LIM, placing more importance on ENSO for driving SWUS hydroclimate than is realistic. Because the LME uses a 2° resolution configuration of CESM1, using CESM1 in this configuration to predict climate change could overemphasize ENSO's influence on future climate variability and change.

By contrast, the ensemble mean correlations are similar between the LIM, CMIP5, and CMIP6-Historical ensembles. Nevertheless, it is also important to focus on the distribution of these correlations. The spread of the GCM correlations is wider than the LIM, and therefore some GCMs simulate unrealistically strong or weak teleconnections. Hence, any attempts to use GCMs for projections should carefully evaluate the role for ENSO in the simulated climate changes.

Our results with the GCMs are consistent with previous studies that found large variability in ENSO teleconnection strengths between models (e.g., Coats et al., 2013; Cook et al., 2016). While there is evidence for improvement in the teleconnection strength in the CMIP6 ensemble, we find that there is still a wide range in the ability of GCMs to simulate ENSO-SWUS teleconnections. Regarding the results from the future climate scenario from

CMIP6, it is important to note that this analysis does not provide a cause for the diminished ENSO-SWUS teleconnection strength in the future. Whether this is simply an effect of the inherent variability that we know exists in the system or an altered teleconnection pattern due to a changing climate, we do not know, and is a question future analysis should answer.

Further process level analysis, particularly of the outliers in correlation in the CMIP5 and CMIP6 ensembles could lend insight into the physical processes most important to realistically simulating the ENSO-SWUS teleconnection. Nevertheless, to robustly determine which of these GCMs best represents the statistics of the real world will require ensembles of each, like the LME, such that the true distribution of correlations can be quantified. In the absence of such ensembles, training LIMs on the climate models themselves may be a useful, though imperfect, path forward (e.g., Coats et al., 2020). Interestingly, two models from CMIP6 included in this analysis are among those considered "too hot" (Hausfather et al., 2022) (CESM2, CanESM2), yet they showed an overall improvement in capturing the ENSO-SWUS teleconnection.

Our results from the LIM are also consistent with previous studies that used observations and reanalysis data to characterize the intrinsic variability in the ENSO-SWUS teleconnection (e.g., McKinnon & Deser, 2018). Where our results differ from the previous literature is in the teleconnection response to a changing climate. In an analysis of GCMs, Yoon et al. (2015) found an increase in extreme hydroclimate events because of a strengthened ENSO in a warmer climate. Yet, predicting future changes to ENSO in a warmer climate remains a difficult task (Cai et al., 2021).

Drought remains an obstacle for water resource managers in the SWUS. Uncertainty in the strength of ENSO teleconnections further complicates water resource management. The SWUS hydroclimate is largely unpredictable from year-to-year. Lack of predictability is particularly problematic when considering that it has been established that lack of water resources has caused the collapse of several civilizations in the SWUS (Benson et al., 2002; Stahle & Dean, 2011). Furthermore, projections exhibit large declines in Colorado River flow in the coming decades (Udall & Overpeck, 2017), which is the main source of water for roughly 60 million Americans in the SWUS. The results from our CMIP6 analysis indicate that the ENSO teleconnection to this region has the potential to decrease in strength, both through intrinsic variability and in response to climate change. Altogether, decreased teleconnection strength and intrinsic variability could mean fewer opportunities for the SWUS to replenish its water stores during El Niños, with potentially dire consequences for stakeholders in the region.

Data Availability Statement

ERSSTV3b data provided by the NOAA PSL, Boulder, Colorado, USA, from their website at https://psl.noaa.gov. CMIP6 data downloaded courtesy of the World Climate Research Programme and Earth System Grid Federation and the Lawrence Livermore National Lab at their website https://esgf-node.llnl.gov and the PDSI data is available via the Terrestrial Hydrology Research Group at Princeton University. The output data from the LIM, and the PDSI data created from the LME, CMIP5, and CMIP6 are available through Cornell University eCommons (https://doi.org/10.7298/8d7j-wt40).

References

Alexander, M. A., Blade, I., Newman, M., Lanzante, J. R., Lau, N. C., & Scott, J. D. (2002). The atmospheric bridge: The influence of ENSO teleconnections on air-sea interaction over the global oceans. *Journal of Climate*, *15*(16), 2205–2231. https://doi.org/10.1175/1520-0442(2002)015<2205:tabtio>2.0.co;2

Alexander, M. A., Matrosova, L., Penland, C., Scott, J. D., & Chang, P. (2008). Forecasting Pacific SSTs: Linear inverse modeling prediction of the PDO. *Journal of Climate*, *21*(2), 385–402. https://doi.org/10.1175/2007jcli1849.1

Allen, R., Pereira, L. S., Raes, D., & Smith, M. (1998). Crop evapotranspiration: Guidelines for computing crop water requirements-FAO Irrigation and Drainage Paper, 56. *Fao, Rome*, *300*(9), D05109.

Ault, T., Cole, J. E., Pederson, G. T., Overpeck, J. T., St. George, S., Otto-Bliesner, B., et al. (2013). The continuum of hydroclimate variability in western North America during the last millennium. *Journal of Climate*, *26*(16), 5863–5878. https://doi.org/10.1175/jcli-d-11-00732.1

Ault, T., Deser, C., Newman, J., & Emile-Geay, J. (2013). Characterizing decadal to centennial variability in the equatorial Pacific during the last millennium. *Geophysical Research Letters*, *40*(13), 3450–3456. https://doi.org/10.1002/grl.50647

Ault, T., George, S., Smerdon, J., Coats, S., Mankin, J. S., Carrillo, C. M., et al. (2018). A robust null hypothesis for the potential causes of megadrought in Western North America. *Journal of Climate*, *31*(1), 3–24. https://doi.org/10.1175/jcli-d-17-0154.1

Benson, L., Kashgarian, M., Rye, R., Lund, S., Paillet, F., Smoot, J., et al. (2002). Holocene multidecadal and multicentennial droughts affecting Northern California and Nevada. *Quaternary Science Reviews*, *21*(4–6), 659–682. https://doi.org/10.1016/s0277-3791(01)00048-8

Cai, W., McPhaden, M. J., Grimm, A. M., Rodriques, R. R., Taschetto, A. S., Garreaud, R. D., et al. (2020). Climate impacts of the El Nino-Southern Oscillation on South America. *Nature Reviews Earth & Environment*, *1*(4), 215–231. https://doi.org/10.1038/s43017-020-0040-3

Cai, W., Santoso, A., Collins, M., Dewitte, B., Karamperidou, C., Kug, J. S., et al. (2021). Changing El Niño-Southern Oscillation in a warming climate. *Nature Reviews Earth & Environment*, *2*(9), 628–644. https://doi.org/10.1038/s43017-021-00199-z

Cai, W., Wang, G., Dewitte, B., Wu, L., Santoso, A., Takahashi, K., et al. (2018). Increased variability of eastern Pacific El Niño under greenhouse warming. *Nature*, *564*(7735), 201–206. https://doi.org/10.1038/s41586-018-0776-9

Cash, B. A., & Burls, N. J. (2019). Predictable and unpredictable aspects of US West Coast rainfall and El Niño: Understanding the 2015/16 event. *Journal of Climate*, *32*(10), 2843–2868. https://doi.org/10.1175/jcli-d-18-0181.1

Chen, C., Cane, M. A., Wittenberg, A. T., & Chen, D. (2017). ENSO in the CMIP5 simulations: Life cycles, diversity, and responses to climate change. *Journal of Climate*, *30*(2), 775–801. https://doi.org/10.1175/jcli-d-15-0901.1

Chen, M., & Kumar, A. (2018). Winter 2015/16 atmospheric and precipitation anomalies over North America: El Niño response and the role of noise. *Monthly Weather Review*, *146*(3), 909–927. https://doi.org/10.1175/mwr-d-17-0116.1

Coats, S., & Karnauskus, K. B. (2017). Are simulated and observed twentieth century tropical Pacific sea surface temperature trends significant relative to internal variability? *Geophysical Research Letters*, *44*(19), 9928–9937. https://doi.org/10.1002/2017gl074622

Coats, S., Smerdon, J., Cook, B., & Seager, R. (2013). Stationarity of the tropical Pacific teleconnections to North America in CMIP5/PMIP3 model simulations. *Geophysical Research Letters*, *40*(18), 4927–4932. https://doi.org/10.1002/grl.50938

Coats, S., Smerdon, J. E., Stevenson, S., Fasullo, J. T., Otto-Bliesner, B., & Ault, T. R. (2020). Paleoclimate constraints on the spatiotemporal character of past and future droughts. *Journal of Climate*, *33*(22), 9883–9903. https://doi.org/10.1175/jcli-d-20-0004.1

Cole, J. E., & Cook, E. R. (1998). The changing relationship between ENSO variability and moisture balance in the continental United States. *Geophysical Research Letters*, *25*(24), 4529–4532. https://doi.org/10.1029/1998gl900145

Cook, B. I., Cook, E. R., Smerdon, J. E., Seager, R., Williams, A. P., Coats, S., et al. (2016). North American megadroughts in the common era: Reconstructions and simulations. *Wiley Interdisciplinary Reviews: Climate Change*, *7*(3), 411–432. https://doi.org/10.1002/wcc.394

Cook, B. I., Williams, A., Mankin, J., Seager, R., Smerdon, J. E., & Singh, D. (2018). Revisiting the leading drivers of Pacific coastal drought variability in the contiguous United States. *Journal of Climate*, *31*(1), 25–43. https://doi.org/10.1175/jcli-d-17-0172.1

Deser, C., Alexander, M. A., Xie, S., & Phillips, A. S. (2010). Sea surface temperature variability: Patterns and mechanisms. *Annual Review of Marine Science*, *2*(1), 115–143. https://doi.org/10.1146/annurev-marine-120408-151453

Deser, C., Simpson, I., Phillips, A., & McKinnon, K. (2018). How well do we know ENSO's climate impacts over North America, and how do we evaluate model accordingly? *Journal of Climate*, *31*(13), 4991–5014. https://doi.org/10.1175/jcli-d-17-0783.1

Deser, C., Simpson, I. R., McKinnon, K. A., & Phillips, A. S. (2017). The Northern Hemisphere extratropical atmospheric circulation response to ENSO: How well do we know it and how do we evaluate models accordingly? *Journal of Climate*, *30*(13), 5059–5082. https://doi.org/10.1175/jcli-d-16-0844.1

DiNezio, P. N., Deser, C., Karspeck, A., Yeager, S., Okumura, Y., Danabasoglu, G., et al. (2017). A 2-year forecast for a 60–80% chance of La Niña in 2017–2018. *Geophysical Research Letters*, *44*(22), 11624–11635. https://doi.org/10.1002/2017gl074904

Enfield, D. B., Mestas-Nuñuz, A. M., & Trimble, P. J. (2001). The Atlantic multidecadal oscillation and its relation to rainfall and river flows in the continental US. *Geophysical Research Letters*, *28*(10), 2077–2080. https://doi.org/10.1029/2000gl012745

Gershunov, A., & Barnett, T. (1998). Interdecadal modulation of ENSO teleconnections. *Bulletin of the American Meteorological Society*, *79*(12), 2715–2725. https://doi.org/10.1175/1520-0477(1998)079<2715:imoet>2.0.co;2

Gupta, V., & Jain, M. K. (2021). Unravelling the teleconnections between ENSO and dry/wet conditions over India using nonlinear Grander causality. *Atmospheric Research*, *247*, 105168. https://doi.org/10.1016/j.atmosres.2020.105168

Hausfather, Z., Marvel, K., Schmidt, G. A., Nielsen-Cammon, J. W., & Zelinka, M. (2022). Climate simulations: Recognize the "hot model" problem. *Nature*, *605*(7908), 26–29. https://doi.org/10.1038/d41586-022-01192-2

Hoerling, M. P., & Kumar, A. (2002). Atmospheric response patterns associated with tropical forcing. *Journal of Climate*, *15*(16), 2184–2203. https://doi.org/10.1175/1520-0442(2002)015<2184:arpawt>2.0.co;2

Hoerling, M. P., Kumar, A., & Zhong, M. (1997). El Nino, La Nina, and the nonlinearity of their teleconnections. *Journal of Climate*, *10*(8), 1769–1786. https://doi.org/10.1175/1520-0442(1997)010<1769:enolna>2.0.co;2

Hu, Q., & Feng, S. (2001). Variations of teleconnections of ENSO and interannual variation in summer rainfall in the central United States. *Journal of Climate*, *14*(11), 2469–2480. https://doi.org/10.1175/1520-0442(2001)014<2469:votoea>2.0.co;2

Jiang, W. P., Huang, P., Huang, G., & Ying, J. (2021). Origins of the excessive westward extension of ENSO SST simulated in CMIP5 and CMIP6. *Journal of Climate*, *34*(8), 2839–2851. https://doi.org/10.1175/jcli-d-20-0551.1

Langenbrunner, B., & Neelin, J. (2013). Analyzing ENSO teleconnections in CMIP models as a measure of model fidelity in simulating precipitation. *Journal of Climate*, *23*(13), 4431–4446. https://doi.org/10.1175/jcli-d-12-00542.1

Larson, S. M., Okumura, Y., Bellomo, K., & Breeden, M. L. (2022). Destructive interference of ENSO on North Pacific SST and North American precipitation associated with Aleutian low variability. *Journal of Climate*, *35*(11), 3567–3585. https://doi.org/10.1175/jcli-d-21-0560.1

Lewis, S. C., & LeGrande, A. N. (2015). Stability of ENSO and its tropical Pacific teleconnections over the last millennium. *Climate of the Past*, *11*(10), 1347–1360. https://doi.org/10.5194/cp-11-1347-2015

Li, X., Hu, Z., Liang, P., & Zhu, J. (2019). Contrastive influence of ENSO and PNA on variability and predictability of North American winter precipitation. *Journal of Climate*, *32*(19), 6271–6284. https://doi.org/10.1175/jcli-d-19-0033.1

McCabe, G. J., Palecki, M. A., & Betancourt, J. L. (2004). Pacific and Atlantic Ocean influences on multidecadal drought frequency in the United States. *Proceedings of the National Academy of Sciences of the United States of America*, *101*(12), 4136–4141. https://doi.org/10.1073/pnas.0306738101

McKinnon, K. A., & Deser, C. (2018). Internal variability and regional climate trends in an observational large ensemble. *Journal of Climate*, *31*(17), 6783–6802. https://doi.org/10.1175/jcli-d-17-0901.1

Meehl, G. A., & Hu, A. (2006). Megadroughts in the Indian monsoon region and southwest North America and a mechanism for associated multidecadal Pacific seas surface temperature anomalies. *Journal of Climate*, *19*(9), 1605–1623. https://doi.org/10.1175/jcli3675.1

Monteith, J. L. (1965). Evaporation and environment. In *19th symposium of the society for experimental biology*, (pp. 205–234). Cambridge University Press.

NADM - North American Drought Monitor. (2022). US drought monitor time series. Retrieved from droughtmonitor.unl.edu

NCEP. (2019). El Niño index dashboard, Niño3.4 time series. Retrieved from esrl.noaa.gov

Newman, M. (2013). An empirical benchmark for decadal forecasts of global surface temperature anomalies. *Journal of Climate*, *26*(14), 5260–5269. https://doi.org/10.1175/jcli-d-12-00590.1

Newman, M., Alexander, M., Ault, T., Cobb, K. M., Deser, C., Di Lorenzo, E., et al. (2016). The Pacific decadal oscillation, revisited. *Journal of Climate*, *29*(12), 4399–4427. https://doi.org/10.1175/jcli-d-15-0508.1

Newman, M., Alexander, M., & Scott, J. (2011). An empirical model of tropical ocean dynamics. *Climate Dynamics*, *37*(9–10), 1823–1841. https://doi.org/10.1007/s00382-011-1034-0

O'Neill, B. C., Tebaldi, C., van Vuuren, D. P., Eyring, V., Friendlingstein, P., Hurtt, G., et al. (2016). The scenario model intercomparison project (scenarioMIP) for CMIP6. *Geosciences Model Development*, *9*, 3461–3482. https://doi.org/10.5194/gmd-9-3461-2016

Otto-Bliesner, B. L., Brady, E. C., Fasullo, J., Jahn, A., Landrum, L., Stevenson, S., et al. (2016). Climate variability and change since 850 CE: An ensemble approach with the Community Earth System Model. *Bulletin of the American Meteorological Society*, *97*(5), 735–754. https://doi.org/10.1175/bams-d-14-00233.1

Penland, C., & Matrosova, L. (1994). A balance condition for stochastic numerical models with application to the El Niño-Southern Oscillation. *Journal of Climate*, *7*(9), 1352–1372. https://doi.org/10.1175/1520-0442(1994)007<1352:abcfsn>2.0.co;2

Penland, C., & Sardeshmukh, P. (1995). The optimal growth of tropical sea surface temperature anomalies. *Journal of Climate*, *8*(8), 1999–2024. https://doi.org/10.1175/1520-0442(1995)008<1999:togots>2.0.co;2

Penman, H. L. (1948). Natural evaporation from open water, bare soil and grass. *Proceedings of the Royal Society of London*, *193*, 120–145. https://doi.org/10.1098/rspa.1948.0037

Perkins, W. A., & Hakim, G. J. (2020). Linear inverse modeling for coupled atmosphere-ocean ensemble climate prediction. *Journal of Advances in Modelling Earth Systems*, *12*(1), e2019MS001778. https://doi.org/10.1029/2019ms001778

Rajagopalan, B., Cook, E., Lall, U., & Ray, B. K. (2000). Spatiotemporal variability of ENSO and SST teleconnections to summer drought over the United States during the twentieth century. *Journal of Climate*, *13*(24), 4244–4255. https://doi.org/10.1175/1520-0442(2000)013<4244:svoeas>2.0.co;2

Redmond, K., & Koch, R. (1991). Surface climate and streamflow variability in the western United States and their relationship to large-scale circulation indices. *Water Resources Research*, *27*(9), 2381–2399.

Schneider, U., Becker, A., Finger, P., Meyer-Christoffer, A., Rudolf, B., & Ziese, M. (2011). GPCC full data reanalysis version 6.0 at 0.5: Monthly land-surface precipitation from rain-gauges built on GTS-based and historic data [Dataset]. GPCC Data Rep. https://doi.org/10.5676/DWD_GPCC/FD_M_V6_050

Sheffield, J., Goteti, G., & Wood, E. F. (2006). Development of a 50-yr high-resolution global dataset of meteorological forcings for land surface modeling. *Journal of Climate*, *19*(13), 3088–3111. https://doi.org/10.1175/jcli3790.1

Singh, S., Abebe, A., Srivastava, P., & Chaubey, I. (2021). Effect of ENSO modulation by decadal and multi-decadal climatic oscillations on contiguous US stream flow. *Journal of Hydrometeorology: Regional Studies*, *36*, 100876. https://doi.org/10.1016/j.ejrh.2021.100876

Smith, T. M., Reynolds, R. W., Peterson, T. C., & Lawrimore, J. (2008). Improvements NOAAs historical merged land-ocean surface temperature analysis (1880–2006). *Journal of Climate*, *21*(10), 2283–2296. https://doi.org/10.1175/2007jcli2100.1

Stahle, D., & Dean, J. (2011). North American tree rings, climatic extremes, and social disasters. *Dendroclimatology*, *11*, 297–327. https://doi.org/10.1007/978-1-4020-5725-0_10

Stevenson, S., Wittenberg, A. T., Fasullo, J., Coats, S., & Otto-Bliesner, B. (2021). Understanding diverse model projections of future extreme El Niño. *Journal of Climate*, *34*(2), 449–464. https://doi.org/10.1175/jcli-d-19-0969.1

Udall, B., & Overpeck, J. (2017). The twenty-first century Colorado River hot drought and implications for the future. *Water Resources Research*, *53*(3), 2404–2418. https://doi.org/10.1002/2016wr019638

Weare, B. (2013). El Niño teleconnections in CMIP5 models. *Climate Dynamics*, *41*(7–8), 2165–2177. https://doi.org/10.1007/s00382-012-1537-3

Williams, A. P., Livnehm, B., McKinnon, K. A., Handsen, W. D., Mankin, J. S., Cook, B. I., et al. (2022). Growing impact of wildfire on Western US water supply. *Proceedings of the National Academy of Sciences of the United States of America*, *119*(10), e2114069119. https://doi.org/10.1073/pnas.2114069119

Yang, S., Li, Z., Yu, J., Hu, X., Dong, W., & He, S. (2018). El Niño-Southern Oscillation and its impact in the changing climate. *National Science Review*, *5*(6), 840–857. https://doi.org/10.1093/nsr/nwy046

Yeh, S., Cai, W., Min, S., McPhaden, M. J., Dommenget, D., Dewitte, B., et al. (2018). ENSO atmospheric teleconnections and their responses to greenhouse gas forcing. *Reviews of Geophysics*, *56*(1), 185–206. https://doi.org/10.1002/2017rg000568

Yoon, J., Wang, S. S., Gillies, R. R., Kravitz, B., Hipps, L., & Rasch, P. J. (2015). Increasing water cycle extremes in California and in relation to ENSO cycle under global warming. *Nature Communications*, *6*(1), 8657. https://doi.org/10.1038/ncomms9657

Zhai, P., Yu, R., Gou, Y., Li, Q., Ren, X., Wang, Y., et al. (2016). The strong El Niño of 2015/16 and its dominant impacts of global and China's climate. *Journal of Meteorological Research*, *30*(3), 283–297. https://doi.org/10.1007/s13351-016-6101-3

Zhang, T., Hoerling, M. P., Wolter, K., Eischeid, J., Cheng, L., Hoell, A., et al. (2018). Predictability and prediction of Southern California rains during strong El Niño events: A focus on the failed 2016 winter rains. *Journal of Climate*, *31*(2), 555–574. https://doi.org/10.1175/jcli-d-17-0396.1

References From the Supporting Information

Herrera, D., & Ault, T. (2017). Insights from a new high-resolution drought atlas for the Caribbean spanning 1950–2016. *Journal of Climate*, *30*(19), 7801–7825. https://doi.org/10.1175/jcli-d-16-0838.1

NOAA_ERSST_V3b. (2019). Data provided by the NOAA/OAR/ESRL PSD. Retrieved from https://www.esrl.noaa.gov/psd/